PNAS RESEARCH ARTICLE | APPLIED BIOLOGICAL SCIENCES

Magnetically powered microwheel thrombolysis of occlusive thrombi in zebrafish

M. Hao Hao Pontius[a], Chia-Jui Ku[a], Matthew J. Osmond[b], Dante Disharoon[b], Yang Liu[a], Mark Warnock[c], Daniel A. Lawrence[c], David W. M. Marr[b], Keith B. Neeves[d,e], and Jordan A. Shavit[a,f,1]

Edited by Leonard Zon, Boston Children's Hospital, Boston, MA; received September 15, 2023; accepted January 9, 2024

Tissue plasminogen activator (tPA) is the only FDA-approved treatment for ischemic stroke but carries significant risks, including major hemorrhage. Additional options are needed, especially in small vessel thrombi which account for ~25% of ischemic strokes. We have previously shown that tPA-functionalized colloidal microparticles can be assembled into microwheels (μwheels) and manipulated under the control of applied magnetic fields to enable rapid thrombolysis of fibrin gels in microfluidic models of thrombosis. Transparent zebrafish larvae have a highly conserved coagulation cascade that enables studies of hemostasis and thrombosis in the context of intact vasculature, clotting factors, and blood cells. Here, we show that tPA-functionalized μwheels can perform rapid and targeted recanalization in vivo. This effect requires both tPA and μwheels, as minimal to no recanalization is achieved with tPA alone, μwheels alone, or tPA-functionalized microparticles in the absence of a magnetic field. We evaluated tPA-functionalized μwheels in CRISPR-generated plasminogen (*plg*) heterozygous and homozygous mutants and confirmed that tPA-functionalized μwheels are dose-dependent on plasminogen for lysis. We have found that magnetically powered μwheels as a targeted tPA delivery system are dramatically more efficient at plasmin-mediated thrombolysis than systemic delivery in vivo. Further development of this system in fish and mammalian models could enable a less invasive strategy for alleviating ischemia that is safer than directed thrombectomy or systemic infusion of tPA.

thrombosis | microparticles | zebrafish | stroke

Significance

Ischemic stroke is caused by pathologic intravascular blood clots (thrombosis) in the brain, resulting in major morbidity and mortality in the developed world. There is only one pharmaceutical treatment, which is dependent on a clot-lysing protein, tissue plasminogen activator (tPA). tPA is either infused systemically or directed using a catheter. However, infusion has a high risk of hemorrhage and catheter-based approaches cannot access the significant proportion of strokes occurring in small vessels. Here, we show that tPA-linked microparticles can be infused into a living organism and induced to assemble μwheels using a magnetic field. This was achieved at much lower tPA concentrations than systemic delivery, thus is a potential therapy to access smaller vessels with lower risk of hemorrhage.

Ischemic stroke occurs in 700,000 people yearly in the United States, which often results in long-term disability (1, 2). Current treatments (3) of ischemic stroke include systemic or catheter-mediated infusion of tissue plasminogen activator (tPA) which can lead to the dissolution of thrombi and subsequent recanalization of occluded vessels. tPA does this by converting plasminogen into plasmin which lyses fibrin (4). Systemic infusion, however, has a limited efficacy window and carries a significant risk of secondary hemorrhage at higher concentrations (1, 5). Catheter-based thrombectomy is another option but is an invasive procedure with its own risks and cannot access small vessels (6, 7). As a result, additional treatment options are needed to minimize these risk factors and improve treatment outcomes, a goal especially important for small vessel thrombi which account for ~25% of ischemic strokes (8).

The promise of micro-scale devices capable of medical intervention has led to the development of microbots that swim, crawl, and roll (9–12). Viscosity plays a dominant role in locomotion at small length scales (13), a factor that microorganisms overcome through physical adaptations, like rotating flagella, that are difficult to artificially replicate and control (14, 15). In a particularly non-biomimetic approach, we have demonstrated a rapid and reversible microbot fabrication and powering method where μm-scale superparamagnetic beads assemble upon application of a relatively weak (1 to 5 mT) rotating magnetic field (16). In this, superparamagnetic beads experience strong attractive interactions, bringing them together to assemble into disc-like shapes we call microwheels (μwheels). These μwheels roll rapidly (100's μm/s) and can be immediately redirected with a simple alteration in the magnetic field orientation resulting in speed and heading changes. Using different time-varying magnetic fields, μwheel size distributions can be created and specific modes specializing in various tasks designed (17). Four unique μwheel modes corresponding to specific needs are discussed here: rolling mode, for optimal mass flux; switchback mode, for steep incline traversal; flipping mode, for deposition of small microbots across a large area; and corkscrew mode, to support burrowing in porous structures.

We have previously shown that μwheels functionalized with tPA enable rapid thrombolysis of fibrin gels and platelet-rich thrombi in vitro by allowing for higher local concentrations of tPA and mechanical burrowing into a thrombus (16, 18). Corkscrew mode demonstrated

Author contributions: M.H.H.P., C.-J.K., M.J.O., D.D., Y.L., M.W., D.A.L., D.W.M.M., K.B.N., and J.A.S. designed research; M.H.H.P., C.-J.K., Y.L., and M.W. performed research; M.H.H.P., C.-J.K., M.J.O., D.D., and M.W. analyzed data; and M.H.H.P., D.A.L., D.W.M.M., K.B.N., and J.A.S. wrote the paper.

Competing interest statement: J.A.S. has been a consultant for Sanofi, Takeda, Genentech, CSL Behring, and HEMA Biologics. D.W.M.M. and K.B.N. are co-inventors on patent US 10,722,250 B2.

This article is a PNAS Direct Submission.

[1]To whom correspondence may be addressed. Email: jshavit@umich.edu.

This article contains supporting information online at https://www.pnas.org/lookup/suppl/doi:10.1073/pnas.2315083121/-/DCSupplemental.

Published February 26, 2024.

superior penetration into fibrin gels compared to rolling mode (16). However, while we were able to achieve local tPA concentrations that were three orders-of-magnitude higher than those reached by diffusive delivery of tPA, this resulted in only a one order-of-magnitude increase in fibrinolysis speed. Based on these results, we showed that there is a biochemical speed limit of fibrinolysis due to plasminogen depletion at high tPA concentrations (19). We have yet to show the efficacy of μwheels for thrombolysis and whether the same plasminogen depletion occurs in vivo.

Zebrafish (*Danio rerio*) is a vertebrate with significant homology to mammalian coagulation systems (20). Development is rapid, external, and embryos and larvae are transparent in the early stages of life (21). This allows for studies using an optical microscope in vivo with intact vasculature, coagulation factors, and blood cells in the context of normal and disrupted hemostasis (22). Here, we show that tPA-functionalized μwheels infused into zebrafish larvae can achieve semi-targeted recanalization in vivo, with the corkscrew mode of translation yielding the fastest recanalization times. Thrombolysis is achieved at three orders-of-magnitude lower overall concentrations compared to tPA infusion and is dependent on plasminogen.

Results

μWheels Facilitate tPA-dependent Recanalization In Vivo. We previously demonstrated that only μwheels functionalized with tPA can achieve lysis of fibrin clots in vitro (18). To test this in vivo, we first infused fluorescently tagged microparticles into circulation at 5 days post fertilization (5 dpf) through the retro-orbital plexus (Fig. 1*A*). After 1 h in circulation, no adverse effects nor any microparticle accumulation in any particular location was observed. We have previously shown the ability to produce occlusive thrombi using laser-mediated endothelial injury in 3 to 5 dpf zebrafish larvae (21), as well as the ability to lyse spontaneous thrombi using human tPA (23). We performed injury prior to microparticle infusion and found accumulation at the upstream edge of the occlusive thrombus (Fig. 1 *B* and *C* and Movie S1). These studies demonstrated that zebrafish larvae tolerate circulation of the beads and that they can be easily visualized.

While, 1 ng of tPA infused into individual larvae is approximately equal to the dosing in patients (0.9 mg/kg) we tested a range of doses, from 1 to 40 ng/larvae, for recanalization. Only high concentrations of tPA, greater than 10 ng/larvae, were able to achieve recanalization within 4 h and without significant toxicity (Fig. 2). Greater concentrations resulted in toxicity evidenced by gross morphologic changes. These studies suggest that, to achieve efficient lysis with minimal toxicity, a high local concentration of tPA is needed.

To test the ability of μwheels to recanalize the vessel, we used microparticles functionalized with recombinant human tPA or Atto-488 fluorescent dye. We used a tPA-specific fluorometric assay to measure the concentration of active tPA bound to the microparticles and calculated that there was approximately 8.4 pg infused per larva. Following endothelial injury, a magnetic field was applied to produce μwheels (Fig. 1 *D*–*F*). All of the larvae with tPA-functionalized μwheels recanalized within 30 min, while control μwheels did not (Fig. 3 and Movies S2–S5). We infused tPA-functionalized microparticles without application of a magnetic field and found no evidence of significant recanalization within 30 min. We also infused non-functionalized particles followed by application of a magnetic field using corkscrew motion. We were only able to apply the magnetic field for 30 min given the heat generated by the coils, but there was no lysis in the absence of tPA. Taken together, these data show that only tPA-functionalized μwheels are capable of thrombolysis.

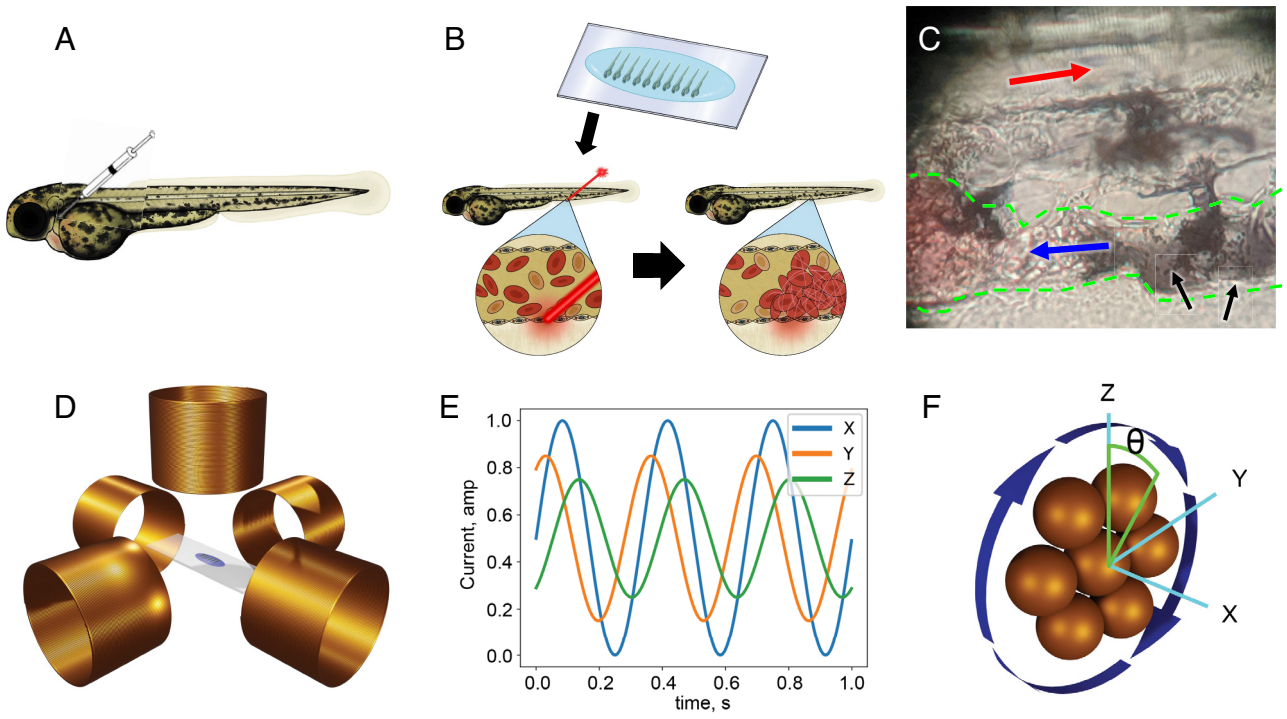

Fig. 1. Generation of μwheels. (*A*) tPA and/or microparticles were infused via the retro-orbital space or PCV using pulled capillary micropipettes. (*B*) 3 dpf zebrafish larvae were mounted in low melting point agarose on glass coverslips and a pulsed dye laser was used to injure the endothelium of the PCV, resulting in thrombosis. (*C*) Photograph of μwheels at the site of a clot. Red and blue arrows indicate the direction of blood flow in the arterial and venous systems, respectively. Black arrows indicate the μwheels at the upstream edge of an occlusive thrombus, outlined with green dashes. (*D*) Zebrafish larvae mounted in low melting point agarose and infused with microparticles were placed in the center of five solenoid coils. (*E*) A laptop running MuControl software connected to a function generator and amplifier sends alternating currents to the x, y, and z coils. (*F*) The rotating magnetic field (blue arrows) induced by the coils causes the assembly and translation of the μwheels with steering controlled by the camber angle (θ) of the field relative to the z-axis.

tPA (ng/larvae)	Number	Toxicity (%)	Fibrinolysis time
0	17	0	> 4 hours
1	16	0	> 4 hours
10	40	0	50-240 min
20	14	60	Sickly, > 4 hours
40	16	100	N/A

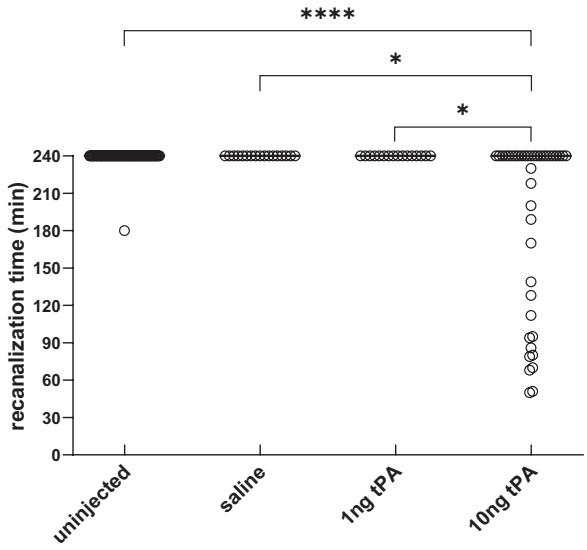

Fig. 2. Time to fibrinolysis after infusion of tPA. The PCV of 3 dpf larvae was injured, producing a completely occluding thrombus. This was followed by either no infusion/uninjected (n = 54), infusion of saline (n = 17), 1 ng of recombinant human tPA (n = 16), or 10 ng of recombinant human tPA (n = 40), and then observation for up to 4 h. Only high concentrations of tPA at 10 ng/larvae (~5 to 10× the amount used for human therapy) were able to achieve recanalization in a fraction of larvae within 4 h and without significant toxicity. Lower concentrations of tPA did not recanalize. Bars represent median recanalization time (*P < 0.01, ****P < 0.0001 by Mantel-Cox log-rank testing).

Corkscrew Motion of μwheels Is Most Effective for Recanalization. The corkscrew motion has been previously shown to be the most effective at lysis in vitro (16). To examine whether this is also the case in vivo, we performed a comparison to additional modes: switchback, flipping, and rolling movements. We compared all of these using tPA-functionalized μwheels and found that corkscrew motion was most effective at recanalizing occlusive thrombi, in a median time of under 10 min. The other modes were also able to recanalize occlusive thrombi within 30 min, but with a median of ~15 min or higher (Fig. 4).

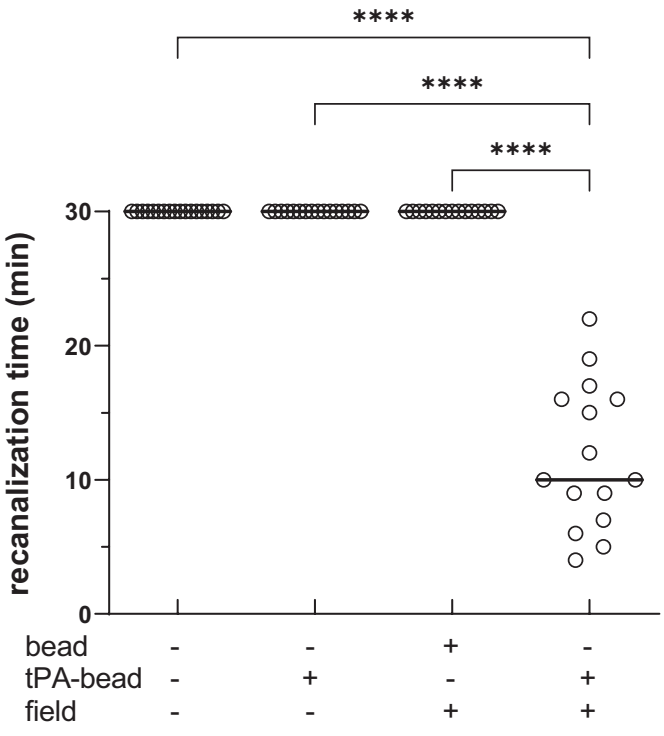

Fig. 3. tPA-functionalized μwheels are necessary for recanalization. The PCV of 3 dpf larvae was injured, producing completely occlusive thrombi, followed by no infusion (n = 18), the infusion of microparticles functionalized with ~8.4 pg of tPA (n = 16), unfunctionalized μwheels (n = 15), or tPA-functionalized μwheels carrying ~8.4 pg of tPA (n = 15). The field was applied in rolling mode either until recanalization was observed or a maximum of 30 min. Beyond that point, the coils became too hot and damaged the larvae. Larvae infused with tPA-functionalized μwheels recanalized within 11.8 ± 5.4 min while those infused with non-functionalized μwheels, tPA-functionalized particles without the application of a magnetic field, and uninfused larvae continued to be occluded after 30 min (P < 0.0001 by Mantel-Cox log-rank testing). Bars represent median recanalization time.

μWheel-mediated Recanalization of Occlusive Thrombi Is Dependent on Plasminogen. tPA is well known to mediate its effects by activating plasminogen to plasmin. Although the plasminogen (*plg*) gene is single copy and conserved in the zebrafish genome, it has not been previously shown whether it has the same function. After endothelial injury, tPA-functionalized microparticles were infused into larvae generated from $plg^{+/-}$ incrosses, followed by application of the magnetic field. μWheels were able to recanalize occlusive thrombi in the majority of wild-type and heterozygous mutants within 30 min, while nearly all of the homozygous mutants were unable to do so (Fig. 5*A*). There was a small significant decrease in the percentage of heterozygous mutants that were able to recanalize compared to wild-type. These data show that fibrinolysis is plasminogen-limited, at least at high local tPA concentrations (19). Finally, when human plasminogen was infused into *plg* mutants, the ability to recanalize was restored (Fig. 5*B*).

Discussion

Within a limited timeframe of 3 to 4.5 h after onset (24), systemic or localized administration of tPA is a current treatment for ischemic stroke which works through the conversion of plasminogen into plasmin, which then effects fibrinolysis. While localized administration is limited to large vessels, systemic delivery has a risk of widespread plasminogen activation, which can result in hemorrhage at high concentrations. A method, therefore, of delivering high concentrations of tPA directly to thrombi while maintaining low systemic concentrations of tPA, could be safer and more effective. In our model, magnetically powered μwheels as a targeted tPA delivery system are dramatically more efficient at plasmin-mediated thrombolysis than systemic administration. In

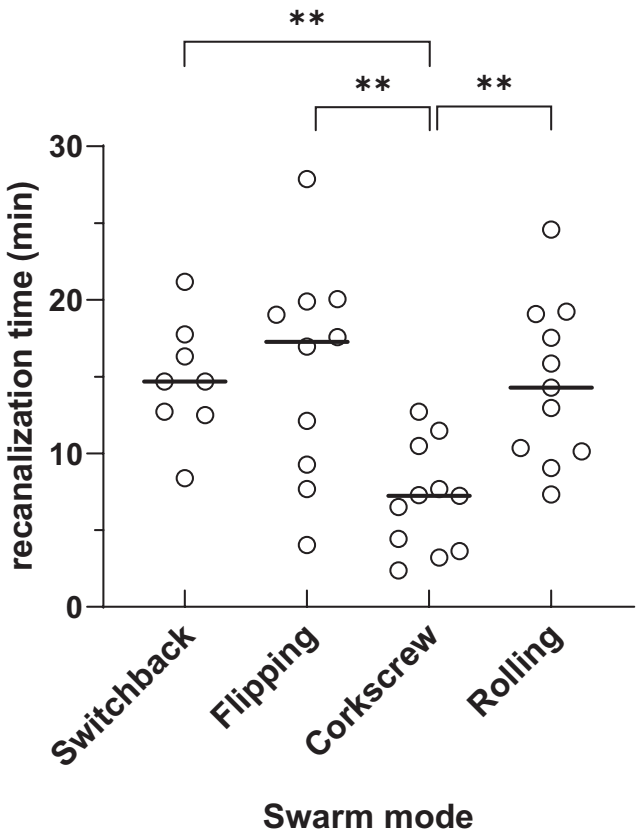

Fig. 4. Effect of motion type on recanalization time. 3 nL of tPA-functionalized μwheels containing ~8.4 pg of tPA were infused into 3 dpf zebrafish larvae following injury causing completely occlusive thrombi. Under switchback (n = 8), flipping (n = 10), or rolling (n = 11) modes of movement all recanalized within 30 min, while μwheels under corkscrew (n = 11) movement recanalized within 15 min (**P < 0.01 by Mantel-Cox log-rank testing). Bars represent median recanalization time.

humans, this approach would enable a less invasive strategy for alleviating ischemic stroke that is safer than directed thrombectomy or systemic infusion of tPA.

We have previously shown that μwheels are effective in uniform in vitro fibrin gels (16). Here, we demonstrate that they can also facilitate thrombolysis in an in vivo system in the context of intact vasculature, coagulation factors, and blood cells. Surprisingly, most of the features are similar. In both systems, tPA-functionalized μwheels are required, and tPA-functionalized microparticles or non-functionalized μwheels are ineffective. Corkscrew motion is also the most efficacious both in vitro and in vivo. Notably, the total concentration of tPA delivered is far lower than the amount needed for lysis using systemic therapy in larvae. With tPA-functionalized μwheels, we were able to decrease the total tPA administered by approximately three orders-of-magnitude compared to larval systemic infusion. We note here that the effective infused tPA concentrations were 10-fold higher than those used in humans, which is similar to doses used in mice (25, 26). However, the relative reduction achieved within the zebrafish model using microparticle delivery provides confidence that similar benefits could be observed in humans.

While the rotating magnetic field controls the assembly and rolling direction of μwheels, we observed that, over time, the particles accumulate in the low-flow regions proximal to the thrombus. This could be due to particle collisions with erythrocytes that similarly drive platelet and leukocytes into low-flow regions (27–29). In species with higher blood flow rates, magnetophoretic forces could be added to direct μwheels/microparticles to the thrombus with electromagnets (30) or with a rotating permanent magnet when significantly higher fields are desired (31). Similarly, removal of residual thrombus material could be achieved by holding tPA-functionalized particles on the vessel wall following recanalization using magnetic fields (32) or by further functionalizing particles with fibrin or platelet-targeted moieties (33).

Using genome editing, we produced a model of plasminogen deficiency. As expected, we were able to confirm that the tPA-functionalized μwheel effects are due to the production of plasmin. Homozygous *plg* mutants had almost no recanalization, verifying conservation of the fibrinolytic system in zebrafish and the ability of human tPA to activate fish plasminogen. Interestingly, we found that there was a dose-dependent response, as heterozygotes had a median recanalization time that was significantly longer than wild-type siblings. This is consistent with plasminogen being the

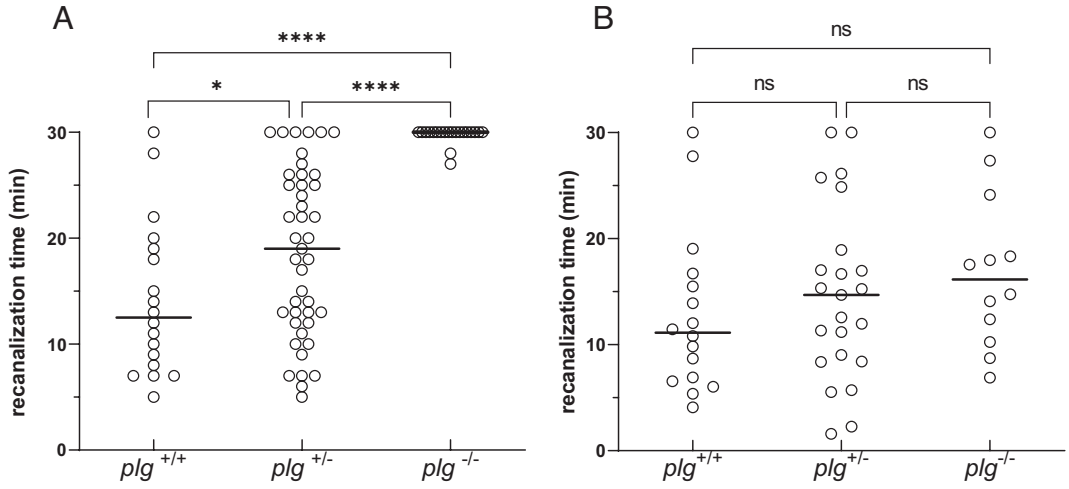

Fig. 5. μWheel-mediated recanalization of occlusive thrombi is dependent on plasminogen. (*A*) CRISPR-mediated genome editing was used to produce a 23 base pair deletion in the *plg* gene. In the majority of wild-type (n = 18) and heterozygous (n = 43) mutants, μwheels were able to recanalize an occlusive thrombus within 30 min. Conversely, the vast majority of homozygous (n = 20) mutants were unable to do so. Interestingly there was a small, but statistically significant decrease in the percentage of heterozygotes that were able to recanalize, when compared to wild-type siblings. (*B*) Plasminogen was infused into *plg* mutant fish [wild-type (n = 16), heterozygous (n = 23), homozygous (n = 12)] and μwheels were able to recanalize the majority of occlusive thrombi within 30 min. Observations were performed prior to genotyping and thus were blinded. Bars represent median recanalization time. (*P < 0.05, ****P < 0.0001 by Mantel-Cox log-rank testing), ns, not significant.

rate-limiting component in local fibrinolysis, as we have previously shown (19). When there is excess tPA, the lytic rate is dictated by available plasminogen. This is consistent with clinical practice and data in which plasminogen levels are correlated with tPA therapeutic success (34, 35).

While zebrafish larvae provide a convenient model for studying the behavior of magnetic-field controlled μwheels, there are limitations to this system. For example, it has allowed the demonstration of recanalization in small capillary-sized vasculature but does not indicate how μwheels would perform in larger caliber vessels. Also, given the limited timeframe that the model allows, residual thrombus remains after recanalization. Finally, zebrafish larvae represent access to superficial, rather than deeper vasculature. Despite this, we show that zebrafish are an effective transitional model between in vitro systems and more complex mammalian models. The results demonstrate a high degree of concordance with microfluidic models, promising a future rapid in vitro to in vivo pipeline.

Materials and Methods

Animal Care. Zebrafish were maintained according to protocols approved by the University of Michigan Animal Care and Use Committee. Wild-type fish were a hybrid line generated from crosses of AB and TL zebrafish acquired from the Zebrafish International Resource Center. Tricaine (Western Chemical) was used for anesthesia and rapid chilling in an ice-water bath for euthanasia in accordance with American Veterinary Medical Association (AVMA) guidelines.

Functionalization of Microparticles. Recombinant tPA was biotinylated using N-hydroxysuccinimide (NHS) activated biotin by incubation on ice for 3 h. Excess biotin was removed using a desalting column, and biotinylated tPA was stored in 20 μL aliquots at −80 °C. 5 μL of 1 μm streptavidin-conjugated iron oxide beads (ThermoFisher Dynabeads MyOne Streptavidin T1) were mixed with biotinylated tPA, incubated at 4 °C overnight, washed three times to remove excess tPA (resulting in negligible free tPA), and resuspended in 15 μL 2% bovine serum albumin (BSA) in saline. Atto 488–biotin was similarly conjugated to Dynabeads without tPA functionalization and used as a control. tPA activity on functionalized beads was measured using the tPA-specific fluorogenic peptide substrate Phe-Gly-Arg-AMC (Centerchem Inc. Norwalk CT) and compared to a standard curve of human tPA. These data indicated that the active tPA concentration of bead slurry was 39.7 nM, which is equivalent to 2.75 pg/nL. Thus, each 3 nL infusion had ~8.4 pg of tPA on ~150 microparticles (~0.056 pg tPA/bead).

Laser-mediated Endothelial Injury Assay. Laser-mediated endothelial injury was performed on 3 dpf zebrafish larvae (21). Larvae were anesthetized in tricaine and mounted in 0.8% low melting point agarose on glass coverslips. The agarose around the head of the larvae was removed and replaced with water. A laser (MicroPoint Pulsed Laser System, Andor Technology, Belfast, Northern Ireland) was used to injure the endothelium of the posterior cardinal vein (PCV) 5 somites caudal to the anal pore using 99 pulses (36).

Infusion of Zebrafish Larvae. After the endothelial injury, 1 to 40 ng tPA or 3 nL (~8.4 pg total tPA) microparticles were infused via retro-orbital vessels using pulled capillary micropipettes (21) (Fig. 1 *A* and *B*). Standard tPA dosage was 0.9 ng/mg [6 dpf larvae have been shown to weigh ~1 mg (37), and 3 dpf is estimated to be 0.5 to 1 mg], corresponding to clinical dosages of 0.9 mg/kg (4, 38). Plasminogen [2 nL of 79 μg/mL solution (Prolytix, Essex Junction, VT)] was infused into *plg* mutants prior to laser injury and infusion of microparticles.

Generation of μwheels. After introduction of the microparticles into the zebrafish larvae, μwheels were assembled using a rotating magnetic field generated with a custom apparatus (39). This apparatus consists of five coils arranged with two opposing pairs in the x and y plane and a fifth coil in the z-direction above the zebrafish sample (Fig. 1*D*). A set of sinusoidal currents are produced by an analog output card (NI-9263, National Instruments, Austin, TX), run through an amplifier (EP2000, Behringer, Willich, Germany), and sent to each pair of coils producing a rotating magnetic field. The circular, rotating magnetic field is positioned normal to the rolling surface, and the direction of the μwheels is manipulated by varying the ratio of current supplied to the individual coils (Fig. 1 *E* and *F*). The magnetic field strength and frequency are controlled with custom software, MuControl (40, 41). Previously, four different magnetic field modes were investigated for controlling μwheel swarms, including switchback, flipping, corkscrew, and rolling (17). Here, we used these modes to investigate their effect on the time to recanalization. Switchback mode results from switching the heading angle of the wheel back and forth which provides better movement over inclined surfaces (Movie S6). Flipping results from changing the camber angle back and forth and provides a way for wheels to prevent assembly into larger wheels (Movie S7). Corkscrew uses a synchronized change in heading angle and camber together that results in enhanced penetration (Movie S8). Rolling is our standard mode in which the heading is fixed manually to control directed movement through complex geometries (Movie S9) (17, 39).

Measurement of Recanalization. Time to recanalization was observed optically for up to 30 min and defined by the resumption of passage of blood cells beyond the occlusive thrombus and into the distal PCV. Longer times were not feasible due to coil heat generation. All observations were collected by an observer blinded to condition or genotype.

CRISPR/Cas9-mediated Genome Editing. We used a CRISPR/Cas9–mediated genome editing system to produce a 23 base pair deletion in the plasminogen (*plg*) gene, as previously described (42). Briefly, single guide RNAs (sgRNAs) were identified using ZiFiT Targeter (43), and sequence GGGAGTACTGCAATATTGAG in exon 12 was selected. DNA templates were produced using pDR274 (44), and sgRNAs transcribed. sgRNAs and Cas9 mRNA were co-injected into one-cell stage zebrafish embryos, at concentrations of 12.5 and 300 ng/μL, respectively. F0 offspring were raised to adulthood and crossed with wild-type zebrafish to verify F1 germline transmission (36). Heterozygotes were incrossed to produce homozygous mutants.

Genotyping of Offspring. Genomic DNA of zebrafish larvae was isolated after incubation in lysis buffer (10 mM Tris-Cl, pH 8.0; 2 mM EDTA, 2% Triton X-100, and 100 μg/mL proteinase K) at 55 °C for 2 h followed by proteinase K inactivation at 95 °C for 5 min. Mutations were detected by PCR using primers 5′-AGATCTAAGGAGAAACCTGT-3′ and 5′-CTTTTTCTGAGGGAGCAGAT-3′.

Statistical Analysis. Statistical analysis was performed with Mantel-Cox log-rank testing. Significance testing was performed using Prism (GraphPad software, CA).

Data, Materials, and Software Availability. All study data are included in the article and/or supporting information.

ACKNOWLEDGMENTS. This work was supported by NIH grants R01 NS102465 to D.W.M.M. and K.B.N., R01-HL055374 to D.A.L., and R35 HL150784 to J.A.S. J.A.S. is the Henry and Mala Dorfman Family Professor of Pediatric Hematology/Oncology.

Author affiliations: [a]Department of Pediatrics, University of Michigan, Ann Arbor, MI 48109; [b]Department of Chemical and Biological Engineering, Colorado School of Mines, Golden, CO 80401; [c]Department of Internal Medicine, University of Michigan, Ann Arbor, MI 48109; [d]Department of Bioengineering, University of Colorado, Denver, Aurora, CO 80045; [e]Department of Pediatrics, University of Colorado, Denver, Aurora, CO 80045; and [f]Department of Human Genetics, University of Michigan, Ann Arbor, MI 48109

1. D. J. Miller, J. R. Simpson, B. Silver, Safety of thrombolysis in acute ischemic stroke: A review of complications, risk factors, and newer technologies. *The Neurohospitalist* **1**, 138–147 (2011).
2. S. J. Mendelson, S. Prabhakaran, Diagnosis and management of transient ischemic attack and acute ischemic stroke: A review. *JAMA* **325**, 1088–1098 (2021).
3. N. Kaneko *et al.*, Devices and techniques. *J. Neuroendovasc. Ther.* **17**, 257–262 (2023).
4. National Institute of Neurological Disorders and Stroke rt-PA Stroke Study Group, Tissue plasminogen activator for acute ischemic stroke. *N Engl. J. Med.* **333**, 1581–1588 (1995).
5. R. Abu Fanne *et al.*, Blood-brain barrier permeability and tPA-mediated neurotoxicity. *Neuropharmacology* **58**, 972–980 (2010).

6. P. Widimsky, L. N. Hopkins, Catheter-based interventions for acute ischaemic stroke. *Eur. Heart J.* **37**, 3081–3089 (2016).
7. M. Gauberti, S. Martinez de Lizarrondo, D. Vivien, Thrombolytic strategies for ischemic stroke in the thrombectomy era. *J. Thromb. Haemost.* **19**, 1618–1628 (2021).
8. S. Sacco *et al.*, A population-based study of the incidence and prognosis of lacunar stroke. *Neurology* **66**, 1335–1338 (2006).
9. R. Dreyfus *et al.*, Microscopic artificial swimmers. *Nature* **437**, 862–865 (2005).
10. P. Erkoc *et al.*, Mobile microrobots for active therapeutic delivery. *Adv. Ther.* **2**, 1800064 (2019).
11. P. L. Venugopalan, B. Esteban-Fernández de Ávila, M. Pal, A. Ghosh, J. Wang, Fantastic voyage of nanomotors into the cell. *ACS Nano* **14**, 9423–9439 (2020).
12. B. Wang, K. Kostarelos, B. J. Nelson, L. Zhang, Trends in micro-/nanorobotics: Materials development, actuation, localization, and system integration for biomedical applications. *Adv. Mater.* **33**, e2002047 (2021).
13. E. M. Purcell, Life at low Reynolds number. *Am. J. Phys.* **45**, 3–11 (1977).
14. J. Wang, Can man-made nanomachines compete with nature biomotors? *ACS Nano* **3**, 4–9 (2009).
15. S. Tottori *et al.*, Magnetic helical micromachines: Fabrication, controlled swimming, and cargo transport. *Adv. Mater.* **24**, 811–816 (2012).
16. T. O. Tasci *et al.*, Enhanced fibrinolysis with magnetically powered colloidal microwheels. *Small* **13**, 1700954 (2017).
17. C. J. Zimmermann, P. S. Herson, K. B. Neeves, D. W. M. Marr, Multimodal microwheel swarms for targeting in three-dimensional networks. *Sci. Rep.* **12**, 5078 (2022).
18. D. Disharoon, D. W. M. Marr, K. B. Neeves, Engineered microparticles and nanoparticles for fibrinolysis. *J. Thromb. Haemost.* **17**, 2004–2015 (2019).
19. D. Disharoon, B. G. Trewyn, P. S. Herson, D. W. M. Marr, K. B. Neeves, Breaking the fibrinolytic speed limit with microwheel co-delivery of tissue plasminogen activator and plasminogen. *J. Thromb. Haemost.* **20**, 486–497 (2022).
20. P. Jagadeeswaran, B. C. Cooley, P. L. Gross, N. Mackman, Animal models of thrombosis from zebrafish to nonhuman primates: Use in the elucidation of new pathologic pathways and the development of antithrombotic drugs. *Circ. Res.* **118**, 1363–1379 (2016).
21. M. S. Rost, S. J. Grzegorski, J. A. Shavit, Quantitative methods for studying hemostasis in zebrafish larvae. *Methods Cell Biol.* **134**, 377–389 (2016).
22. C. A. Kretz, A. C. Weyand, J. A. Shavit, Modeling disorders of blood coagulation in the zebrafish. *Curr. Pathobiol. Rep.* **3**, 155–161 (2015).
23. Y. Liu *et al.*, Targeted mutagenesis of zebrafish antithrombin III triggers disseminated intravascular coagulation and thrombosis, revealing insight into function. *Blood* **124**, 142–150 (2014).
24. M. G. Lansberg, E. Bluhmki, V. N. Thijs, Efficacy and safety of tissue plasminogen activator 3 to 4.5 hours after acute ischemic stroke: A meta-analysis. *Stroke* **40**, 2438 (2009).
25. A. Goncalves *et al.*, Thrombolytic tPA-induced hemorrhagic transformation of ischemic stroke is mediated by PKCβ phosphorylation of occludin. *Blood* **140**, 388–400 (2022).
26. D. Torrente *et al.*, Compartmentalized actions of the plasminogen activator inhibitors, PAI-1 and Nsp, in Ischemic Stroke. *Transl. Stroke Res.* **13**, 801–815 (2022).
27. T. Karino, H. L. Goldsmith, Adhesion of human platelets to collagen on the walls distal to a tubular expansion. *Microvasc. Res.* **17**, 238–262 (1979).
28. C. Skilbeck, S. M. Westwood, P. G. Walker, T. David, G. B. Nash, Dependence of adhesive behavior of neutrophils on local fluid dynamics in a region with recirculating flow. *Biorheology* **38**, 213–227 (2001).
29. M. Lehmann *et al.*, Platelets drive thrombus propagation in a hematocrit and glycoprotein VI–Dependent manner in an in vitro venous thrombosis model. *Arterioscler. Thromb. Vasc. Biol.* **38**, 1052–1062 (2018).
30. D. Disharoon, K. B. Neeves, D. W. M. Marr, ac/dc magnetic fields for enhanced translation of colloidal microwheels. *Langmuir* **35**, 3455–3460 (2019).
31. C. J. Zimmermann, A. Petruska, K. B. Neeves, D. W. M. Marr, Coupling magnetic torque and force for colloidal microbot assembly and manipulation. *Adv. Intell. Syst.* **5**, 2300332 (2023).
32. A. Nacev, C. Beni, O. Bruno, B. Shapiro, The behaviors of ferromagnetic nano-particles in and around blood vessels under applied magnetic fields. *J. Magn. Magn. Mater.* **323**, 651–668 (2011).
33. S. Absar, N. Gupta, K. Nahar, F. Ahsan, Engineering of plasminogen activators for targeting to thrombus and heightening thrombolytic efficacy. *J. Thromb. Haemost.* **13**, 1545–1556 (2015).
34. M. J. Manco-Johnson, How I treat venous thrombosis in children. *Blood* **107**, 21–29 (2006).
35. M. Andrew, L. Brooker, M. Leaker, B. Paes, J. Weitz, Fibrin clot lysis by thrombolytic agents is impaired in newborns due to a low plasminogen concentration. *Thromb. Haemost.* **68**, 325–330 (1992).
36. A. C. Weyand *et al.*, Analysis of factor V in zebrafish demonstrates minimal levels needed for early hemostasis. *Blood Adv.* **3**, 1670–1680 (2019).
37. K. Dabrowski, M. Miller, Contested Paradigm in Raising Zebrafish (Danio rerio). *Zebrafish* **15**, 295–309 (2018).
38. A. B. Nair, S. Jacob, A simple practice guide for dose conversion between animals and human. *J. Basic Clin. Pharm.* **7**, 27–31 (2016).
39. E. J. Roth *et al.*, An experimental design for the control and assembly of magnetic microwheels. *Rev. Sci. Instrum.* **91**, 093701 (2020).
40. C. Zimmermann, czimm79/MuControl: v1.1.1–DOI Generation (2021). https://doi.org/10.5281/zenodo.5793922 (2 June 2023).
41. M. J. Osmond *et al.*, Magnetically powered chitosan milliwheels for rapid translation, barrier function rescue, and delivery of therapeutic proteins to the inflamed gut epithelium. *ACS Omega* **8**, 11614–11622 (2023).
42. A. C. Weyand, J. A. Shavit, Zebrafish as a model system for the study of hemostasis and thrombosis. *Curr. Opin. Hematol.* **21**, 418–422 (2014).
43. W. Y. Hwang *et al.*, Efficient genome editing in zebrafish using a CRISPR-Cas system. *Nat. Biotechnol.* **31**, 227–229 (2013).
44. W. Y. Hwang *et al.*, Heritable and precise zebrafish genome editing using a CRISPR-Cas system. *PLoS One* **8**, e68708 (2013).